PHILOSOPHICAL TRANSACTIONS B

royalsocietypublishing.org/journal/rstb

Research

Cite this article: Lu L, Wang Q, Huang D, Xu Q, Zhou X, Wu J. 2019 Rice black-streaked dwarf virus P10 suppresses protein kinase C in insect vector through changing the subcellular localization of LsRACK1. *Phil. Trans. R. Soc. B* **374**: 20180315.
http://dx.doi.org/10.1098/rstb.2018.0315

Accepted: 26 November 2018

One contribution of 19 to a theme issue 'Biotic signalling sheds light on smart pest management'.

Subject Areas:
plant science, microbiology

Keywords:
rice black-streaked dwarf virus, P10 protein, *Laodelphax striatellus*, receptor for activated protein C kinase 1, RACK1, protein kinase C

Authors for correspondence:
Jianxiang Wu
e-mail: wujx@zju.edu.cn
Xueping Zhou
e-mail: zzhou@zju.edu

†These authors contributed equally to this study.

Electronic supplementary material is available online at https://dx.doi.org/10.6084/m9.figshare.c.4326044.

THE ROYAL SOCIETY PUBLISHING

Rice black-streaked dwarf virus P10 suppresses protein kinase C in insect vector through changing the subcellular localization of LsRACK1

Lina Lu[1,†], Qi Wang[1,†], Deqing Huang[1], Qiufang Xu[2], Xueping Zhou[1,3] and Jianxiang Wu[1]

[1]State Key Laboratory of Rice Biology, Institute of Biotechnology, Zhejiang University, Hangzhou, Zhejiang 310058, People's Republic of China
[2]Institute of Plant Protection, Jiangsu Academy of Agricultural Sciences, Nanjing 210014, People's Republic of China
[3]State Key Laboratory for Biology of Plant Diseases and Insect Pests, Institute of Plant Protection, Chinese Academy of Agricultural Sciences, Beijing 100193, People's Republic of China

XZ, 0000-0001-5311-7331; JW, 0000-0002-7611-7833

Rice black-streaked dwarf virus (RBSDV) was known to be transmitted by the small brown planthopper (SBPH) in a persistent, circulative and propagative manner in nature. Here, we show that RBSDV major outer capsid protein (also known as P10) suppresses the protein kinase C (PKC) activity of SBPH through interacting with the receptor for activated protein kinase C 1 (LsRACK1). The N terminal of P10 (amino acids (aa) 1–270) and C terminal of LsRACK1 (aa 268–315) were mapped as crucial for the interaction. Confocal microscopy and subcellular fractionation showed that RBSDV P10 fused to enhanced green fluorescent protein formed vesicular structures associated with endoplasmic reticulum (ER) membranes in *Spodoptera frugiperda* nine cells. Our results also indicated that RBSDV P10 retargeted the initial subcellular localization of LsRACK1 from cytoplasm and cell membrane to ER and affected the function of LsRACKs to activate PKC. Inhibition of RACK1 by double stranded RNA-induced gene silencing significantly promoted the replication of RBSDV in SBPH. In addition, the PKC pathway participates in the antivirus innate immune response of SBPH. This study highlights that RACK1 negatively regulates the accumulation of RBSDV in SBPH through activating the PKC signalling pathway, and RBSDV P10 changes the subcellular localization of LsRACK1 and affects its function to activate PKC.

This article is part of the theme issue 'Biotic signalling sheds light on smart pest management'.

1. Introduction

Rice black-streaked dwarf virus (RBSDV) causes devastating diseases in rice and maize fields in China and Japan [1]. RBSDV belongs to the genus *Fijivirus*, family Reoviridae, and can be transmitted by *Laodelphax striatellus* (small brown planthopper, SBPH) in a persistent and circulative-propagative manner [1,2]. The RBSDV genome consists of 10 linear double-stranded RNAs (dsRNAs) and encodes thirteen proteins. Each dsRNA has one open reading frame (ORF) except RNA S5, S7 and S9 (two ORFs each) [3–5]. To date, the P6 protein has been shown to be an RNA silencing suppressor [6] and P7-1 was reported to form tubules in insect cells to facilitate virus spread from the midgut epithelium into the visceral circular muscle through the basal lamina, similar to that reported for southern rice black-streaked dwarf virus (SRBSDV) [7,8]. Protein P9-1 was shown to form viroplasm-like structures by itself in *Arabidopsis* protoplasts or in *Spodoptera frugiperda* 9 (Sf9) cells [9,10]. The P10 protein is known to be the viral major outer capsid protein (P10) with 558 amino acids and a molecular

weight of about 63 kDa. Bioinformatic analyses revealed that RBSDV P10 has three predicted transmembrane domains (TM1, TM2 and TM3) [11]. It was reported that transient expression of RBSDV P10 fused to an enhanced green fluorescent protein (eGFP) in *Nicotiana benthamiana* epidermal cells or in rice protoplasts formed endoplasmic reticulum (ER)-associated vesicular-like structures [11]. More recent studies have indicated that the viral P10 is multifunctional and may function in almost every stage during virus infection in plants through specific interactions with other viral and/or host factors [12].

Insects have evolved effective antivirus innate immune responses, including humoral and cellular responses [13]. Humoral immune responses include synthesizing antimicrobial peptides, triggering enzymatic cascades that regulate coagulation, melanizing foreign materials in haemolymph, and producing reactive oxygen or nitrogen species [14]. Cellular-mediated immune responses include phagocytosis, nodulation, encapsulation and melanization [15]. To escape insect host immune responses, viruses have evolved strategies to avoid to be targeted by these immune responses [16].

The receptor for activated C kinase 1 (RACK1) is a 36 kDa protein with seven repeated tryptophan-aspartate (WD) domains and can form a propeller-like structure acting as a intracellular scaffold protein involved in many signalling events [17,18]. RACK1 was originally identified as a receptor for protein kinase C (PKC) members in mammals [19,20]. In animals, RACK1 is known as a multifunctional protein, important for its roles in regulating several cell surface receptors and intracellular protein kinases [21]. RACK1 was demonstrated to localize at the internal side of membranes and on cytoskeletons in cytosol [22,23]. RACK1 can bind to and stabilize PKCs to increase PKC-mediated phosphorylation. Sequences of RACK1 from yeast, plants and animals were highly conserved [24].

PKC is a multimember protein kinase family involved in regulating functions of many other proteins through phosphorylating the hydroxyl groups on serine and threonine amino acid residues. PKC itself can be activated by signalling molecules, such as increased concentrations of diacylglycerol or calcium ions (Ca^{2+}) [25]. PKC enzymes are known to play important roles in several signal transduction cascades [26]. Previous reports have indicated that RACK1 can bind with PKCs and activate them to serve as an intracellular receptor, which anchors activated PKCs to cytoskeleton, and targets PKCs to membranes [22,23]. In addition to the above activities, PKCs were shown to regulate virus endocytic trafficking through phosphorylation [27]. Interaction of PKC with RACK1 is thought not only to target PKC to proper intracellular locations but also to hold PKC in an active conformation [28]. This model is based on the premise that the PKC isoforms that are capable of interacting with RACK1 all contain a pseudo-RACK1 binding site within its primary amino acid sequence [20]. PKC contains a pseudo-substrate sequence in the regulatory domain of PKC that binds to the substrate site to maintain the enzyme in the inactive form [20]. RACK1 can disrupt these interactions and stabilize the bound PKC in an open and active conformation [20,28].

Numerous viruses can be transmitted by insect vectors [29]. However, the molecular mechanism controlling virus transmission by insect vector was poorly understood [30]. To better understand the biological functions of viral capsid protein during virus transmission, we investigated the interaction between RBSDV P10 and its insect vector factors. The result of this study demonstrated that RBSDV P10 interacted with LsRACK1 of *L. striatellus* both *in vivo* and *in vitro*. Although previous reports had shown that RACK1 could bind with rice stripe virus (RSV) or beet western yellow virus (BWYV) particles, based on two-dimensional electrophoresis (2-DE), the nature of protein(s) on virus particles that interacted specifically with RACK1 were unclear [31,32]. In this study, we further investigated the roles of LsRACK1 and the PKC cascade during RBSDV transmission by *L. striatellus*. Our results demonstrated that LsRACK1 and the PKC cascade have negative effects on RBSDV accumulation in the insect vector. These new findings provide useful information on the molecular mechanism by which *Fijivirus* interacts with its insect vectors.

2. Material and methods

(a) Virus resource, host plant and insect care

RBSDV Kaifeng isolate was obtained from an infected rice plant in a field in the Henan Province, China. The virus was characterized through reverse transcription-polymerase chain reaction (RT-PCR) using specific primers and serological assays using an anti-RBSDV monoclonal antibody [33]. RBSDV in this plant was transmitted to new rice seedlings by *L. striatellus* Fallen and the infected plants were maintained in an insect-free greenhouse until further use. *Laodelphax striatellus* was maintained on rice seedlings in an insect culture room as described previously [31]. Briefly, non-viruliferous *L. striatellus* were allowed to grow on rice seedlings cv. Huainan No. 5 in large glass beakers covered with a layer of nylon mesh inside an insect growth room, set at 25°C and a 16 L : 8 D photoperiod cycle. Rice seedlings were changed once every 10–14 days.

(b) Vector construction and yeast two-hybrid assay

The RBSDV *P10* gene was amplified from the total RNA extracted from a RBSDV-infected rice plant through RT-PCR and cloned into the pGBKT7 (BD) vector (Clontech, Mountain View, CA, USA) to generate a bait vector pGBKT7-P10 (BD-P10). Construction and screening of an *L. striatellus* cDNA library was conducted as instructed by the manufacturer (Clontech). Full-length sequence of the *LsRACK1* gene of *L. striatellus* was obtained through searching the database at the National Center for Biotechnology Information (www.ncbi.nlm.nih.gov/pubmed). The coding sequence of *LsRACK1* was then PCR-amplified from an *L. striatellus* cDNA and inserted into the pGADT7 (AD) or BD vector. The coding sequences of RBSDV *P10* deletion mutant (muP10) or *LsRACK1* deletion mutant (muRACK1) was also RT-PCR amplified with specific primers and cloned individually into the vector AD or BD. The muP10 mutants were made based on the predictions of their transmembrane domains using online software (http://www.cbs.dtu.dk/services/TMHMM/). The muRACK1 mutants were made based on the prediction of its seven WD40 domains. Primers used in this study are listed in the electronic supplementary material, table S1 and the authenticity of each construct was confirmed through DNA sequencing.

Analysis of protein–protein interaction in yeast was performed as described previously [34]. Briefly, combinations of two different plasmids were transformed into *Saccharomyces cerevisiae* strain Gold. *Saccharomyces cerevisiae* transformed with pGADT7-T (AD-T, encoding simian virus 40 (SV40) large T antigen) and pGBKT7-p53 (BD-p53), AD-T and pGBKT7-Lamin (BD-Lam, encoding human lamin C protein), or BD and AD empty vectors were used as the positive, negative and blank negative controls, respectively. The transformed *S. cerevisiae* cells were grown at 30°C for 72 h on a triple-selective medium (SD-LTH/3-AT/Aba, lacking leucine, tryptophan and histidine, supplemented with 25 mM 3-amino-1,2,4-triazole (3-AT) and 70 ng ml^{-1} aureobasidin

A (Aba)), or on a quadruple-selective medium (SD-LTHA/Aba, lacking leucine, tryptophan, histidine and adenine, supplemented with 70 ng ml^{-1} Aba).

(c) Protein analysis, co-immunoprecipitation assay and glutathione S-transferases pull-down assay

For protein expression analyses, total protein was extracted from *L. striatellus* tissues or Sf9 cells in a 2×sodium dodecyl sulfate-polyacrylamide gel electrophoresis (SDS-PAGE) loading buffer (1 : 1, w/v, mg ml^{-1}). After 10 min boiling, the total protein extracts were separated in SDS-PAGE gels through electrophoresis. The separated proteins were transferred to nitrocellulose membranes followed by detections of specific proteins using indicated antibodies. For co-immunoprecipitation (Co-IP) assay, total protein was extracted from Sf9 cells in ice-cold immunoprecipitation buffer (25 mM Tris, pH 7.5, containing 10% glycerol (v/v), 0.15% nonidet P-40 (v/v), 150 mM NaCl and 1 × protease inhibitor cocktail (Roche)). Protein extracts were incubated with a Myc antibody for 2 h at 4°C, and then incubated with protein A/G beads for 4 h at 4°C. The precipitated proteins were washed three times with ice-cold immunoprecipitation buffer at 4°C and analysed by Western blot using an anti-Myc or an anti-HA antibody (Abcam).

Based on the results from the protein–protein interaction assays in yeast, a full-length *LsRACK1* gene was PCR-amplified and cloned into the pGEX4T-3 vector to express glutathione S-transferases (GST)-tagged LsRACK1 fusion protein in *Escherichia coli* strain BL21 (DE3). A 6X His-P10-HA fusion protein was expressed in Sf9 cells. The GST-LsRACK1 protein was purified using a GST-bind resin (Novagen) and the 6X His-P10-HA fusion protein was purified using a Ni-NTA His*bind resin (Novagen) as instructed by manufacturers. Approximately 1 mg of individual purified GST fusion protein or GST was incubated with 1 mg 6X His-P10-HA fusion protein at 4°C for 3 h in 1 ml buffer A (50 mM Tris–HCl, pH 7.5, containing 100 mM NaCl, 0.1 mM EDTA, 0.1 mM EGTA, 0.2% Triton X-100, 0.1% β-mercaptoethanol, 1 mM PMSF and protease inhibitor cocktail). The beads were washed three times with ice-cold buffer B (50 mM HEPES, pH 7.5, 100 mM NaCl, 0.1 mM EDTA, 1 mM PMSF and protease inhibitor cocktail) at 4°C. The washed beads were boiled for 10 min in 2x SDS-PAGE loading buffer and the proteins were separated in SDS-PAGE gels followed by Western blot using an anti-HA antibody.

(d) Baculovirus expression assay

DNA fragments representing full-length RDSDV *P10*, *LsRACK1* or various deletion mutants were PCR-amplified. The resulting PCR products were purified and inserted individually into vector pFastBac (Invitrogen, Carlsbad, CA, USA). The recombinant baculovirus vectors were introduced individually into *E. coli* DH10Bac cells (Invitrogen) prior to transposition into the bacmid vector. The recombinant bacmid vectors were then individually used to transfect Sf9 cells in the presence of cellfectin. The transfected cells were incubated inside a 27°C humidified incubator for 72 h. The baculovirus expression assays were performed as instructed (Invitrogen). The cells expressing protein were examined using an inverted Zeiss LSM780 confocal laser-scanning microscope (Zeiss, Göttingen, Germany) and the images were processed using ZEN software (Zeiss).

(e) Immunofluorescence microscopy

Midguts, ovaries and testes were dissected from non-viruliferous and viruliferous *L. striatellus* in cold distilled water on a glass plate, and fixed in 4% paraformaldehyde for 2 h at room temperature (RT). After being permeabilized with osmotic buffer (0.01 M phosphate-buffered saline (PBS) containing 2% Triton X-100, pH 7.4) for 4 h, the tissues were blocked with 1% bovine serum albumin for 30 min at RT. The samples were probed with an anti-RBSDV P10 murine monoclonal antibody conjugated with fluorescein isothiocyanate (FITC), and an anti-LsRACK1 rabbit polyclonal antibody, overnight at 4°C. After washing with 0.01 M PBS containing 1% Tween-20 (pH 7.4), the tissues were incubated in a goat anti-rabbit IgG conjugated with Alexa Flour 555 (Sangon Biotech) for 2 h at room temperature. Nuclei in cells were stained blue using DAPI (Beyotime Biotechnology) in accordance with the manufacturer's instructions. The images were viewed under an inverted Zeiss LSM780 confocal laser-scanning microscope (Zeiss). Thirty copies of each treatment were tested.

(f) Subcellular fractionation through sucrose gradient centrifugation

Subcellular fractionation was conducted as previously described [35] with minor modifications. Briefly, at 48 h post-transfection, Sf9 cells were washed twice in ice-cold 0.01 M PBS, pelleted, resuspended in PBS containing 10 mM EDTA and incubated at 4°C for 5–10 min. The cells were pelleted, resuspended in ice-cold PBS and pelleted again. The resulting cells were resuspended in a hypotonic buffer (10 mM Tris–HCl, pH 7.4, 1 mM EDTA) supplemented with complete mini protease inhibitor cocktail as instructed (1 tablet/10 ml buffer, Roche Applied Science, Mannheim, Germany), kept at −80°C for about 30 min, and then allowed the cells to swell at RT for 15–20 min. The cells were disrupted by sonication. The suspensions were added to NaCl to a final concentration of 150 mM, and centrifuged at 1000*g* for 10 min at 4°C to remove cell debris. SDS was added to the supernatant to reach a final concentration of 0.1%. The supernatant (300 µl) was mixed with 1.6 ml 80% (w/v) sucrose solution and placed underneath a layer of 65% sucrose (7.0 ml) inside a centrifuge tube. The top layer was 3.1 ml 10% sucrose. After centrifugation at 151 000*g* for 4 h at 4°C, the sample was fractionated nine equal parts (1.5 ml per fraction) starting from the top of the centrifuge tube. The membrane-associated vesicles were floated in the 65% and 10% sucrose gradients. Each fraction was subjected to Western blot analysis.

(g) Double stranded RNAs preparation and transfection of *Spodoptera frugiperda* 9 cells

DsRNAs were synthesized using the MEGAscript T7 Transcription Kit (catalogue no. AM1333, Ambion, Austin, TX, USA). Briefly, DNA fragments used for productions of dsRNAs were PCR-amplified using specific primers with a T7 RNA polymerase promoter sequence (electronic supplementary material, table S1). A 414 bp segment representing a partial sequence of *GFP* gene was also PCR-amplified and used as a control. The resulting DNA fragments were used (200 ng per reaction) to produce dsRNAs. The synthesized dsRNAs were concentrated via LiCl precipitation and then resuspended in nuclease-free water. Quality and size of the dsRNAs were visualized in 1% agarose gels after electrophoresis. Sf9 cells were transfected with dsRNAs (0.5 µg $µl^{-1}$) in the presence of cellfectin as instructed and gene silence efficiency was determined at 72 h post transfection through real-time quantitative RT-PCR (qRT-PCR) and Western blot.

(h) Quantification of rice black-streaked dwarf virus proliferation in RNA interference planthoppers

Microinjection of dsRNA into *L. striatellus* was performed as previously reported [36]. Second-instar *L. striatellus* nymphs were randomly collected from the *L. striatellus* culture and anaesthetized with CO_2 for 30 s. For LsRACK1 knockdown,

approximately 25 ng dsRNA was injected into the thorax between the mesocoxa and the hind coxa using a FemtoJet microinjection system (Eppendorf, Hauppauge, NY, USA). A total of 200–250 nymphs were injected for each treatment. At 4 h post-injection, the nymphs were allowed to feed on RBSDV-infected rice plants for 3 d and then on healthy rice seedlings. To determine the efficiency of *LsRACK1* silencing, total RNA was extracted from 20 individual nymphs at 2 d post microinjection and analysed through qRT-PCR. The remaining nymphs were allowed to continue to feed on the RBSDV-infected rice plants for one more day and then on healthy rice seedlings for 15 d. The resulting nymphs were used to determine the effect of *LsRACK1* silencing on RDSDV *P10* gene expression by qRT-PCR and Western blot.

Total RNA was isolated from *L. striatellus* using TRIzol reagent (Invitrogen). Rever Tra Ace® qPCR RT Master Mix with gDNA remover was used to conduct reverse transcription as instructed (Toyobo, Osaka, Japan). RT-PCR and qRT-PCR were performed as described previously [37]. All primers used in assays are described in the electronic supplementary material, table S1. Specific primers for qRT-PCR were designed using the Primer Premier 5 software.

(i) Measurement of protein kinase C activity

Microinjection of 10 µl 1 µM PKCs specific inhibitor Calphostin C (Sigma-Aldrich, Santa Clara, CA, USA) or 1 µM PKCs activator phorbol-12-myristate-13-acetate (PMA) (Sigma-Aldrich) into *L. striatellus* was performed to suppress or activate the PKC activity as previously reported [38]. Planthopper tissues or cell lysate were assayed for PKC activity using the PepTag® Non-Radioactive PKC Assay kit as instructed (Promega, Madison, WI, USA). Briefly, 0.1 g tissue or 5×10^6 to 1×10^7 cultured Sf9 cells were homogenized in 0.5 ml cold PKC extraction buffer (25 mM Tris–HCl, pH 7.4, 0.5 mM EDTA, 0.5 mM EGTA, 0.05% Triton X-100, 10 mM β-mercaptoethanol, 1 µg ml^{-1} leupeptin, 1 µg ml^{-1} aprotinin, 0.5 mM PMSF) using a cold homogenizer. The homogenates were centrifuged at 14 000*g* for 5 min at 4°C in a micro-centrifuge tube and the pellets were discarded. Reaction reagent was made by mixing 5 µl PepTag® PKC reaction 5X buffer, 5 µl PepTag® C1 peptide, 5 µl sonicated PKC activator 5X solution and 8 µl water in a 0.5 ml micro-centrifuge tube set on ice as instructed by the manufacturer. The tube was incubated in a 30°C water bath for 2 min followed by addition of 2 µl supernatant described above or PKC. The mixed samples were incubated again at 30°C for 30 min followed by boiling the sample for 2 min or by heating the sample in a 95°C heating block for 10 min to stop the reaction. For electrophoresis, 1 µl 80% glycerol was added to each sample prior to loading the samples into wells in 0.8% agarose gels to ensure all the samples remained in the wells. The activity of PKC in each sample was calculated based on the content of the phosphorylated substrate. Statistical significance between the two treatments was determined using Student's *t*-test and $p < 0.05$ was considered to be statistically significant.

3. Results

(a) Interaction between rice black-streaked dwarf virus P10 and LsRACK1

RBSDV P10 was used as a bait to screen a *L. striatellus* cDNA library by yeast two-hybrid (Y2H) assay. From this assay, a 687 bp DNA fragment showing 94% nucleotide sequence similarity with a *L. striatellus* gene, i.e. *LsRACK1* (nucleotide position 262–948) was identified. Subsequently, a full-length coding sequence for *LsRACK1* was cloned using specific primers. Sequence analysis revealed that the full-length *LsRACK1* ORF contains 948 nucleotides (nt) (GenBank accession No. HQ385972.1) and encodes a protein with 315 amino acids (aa) with seven WD40 domains, which has high homology with that of *Sogatella furcifera* Horváth and *Nilaparvata lugens* (figure 1*a*,*b*).

RBSDV P10 and LsRACK1 fusion expression vectors with either a GAL4 activation domain (e.g. AD-LsRACK1) or a GAL4 DNA binding domain (e.g. BD-P10) were constructed. *Saccharomyces cerevisiae* cultures co-transfected with various combinations of two different vectors were plated on the SD-LTH/3-AT/Aba or SD-LTHA/Aba medium to determine the activation of reporter genes. Results showed that yeast harbouring both AD-P10 and BD-LsRACK1 or AD-T and BD-p53 vectors were able to grow on both SD-LTH/3-AT/Aba and SD-LTHA/Aba media (figure 1*c*). Yeast harbouring both BD-P10 and AD-LsRACK1 or AD-LsRACK1 and the empty GAL4 DNA binding domain vector (BD) were able to grow on the SD-LTH/3-AT/Aba medium but not the SD-LTHA/Aba medium (figure 1*c*). Yeast harbouring AD and BD-LsRACK1, AD-P10 and BD, BD-P10 and AD or AD-T and BD-Lam were unable to proliferate on both media (figure 1*c*), suggesting that RBSDV P10 did interact with LsRACK1 after been expressed in yeast.

To further confirm the above Y2H results, we further analysed the interaction between RBSDV P10 and LsRACK1 using a Co-IP assay. The HA-tagged P10 (P10-HA) and the Myc-tagged LsRACK1 (LsRACK1-Myc) were expressed individually or together in Sf9 cells. Cell lysates from different treatments were collected at 48 h post transfection and total protein extracts were analysed through Co-IP using anti-Myc antibody coupled agarose beads. The resulting precipitates were analysed by Western blot using an anti-HA antibody. The result indicated that RBSDV P10 was indeed co-immunoprecipitated with LsRACK1-Myc (figure 1*d*).

We then tested the interaction between RBSDV P10 and LsRACK1 *in vitro* by GST pull-down assay. The GST-tagged LsRACK1 (GST-LsRACK1) was expressed in *E. coli* and the double-tagged RBSDV P10 (6X His-P10-HA) was expressed in Sf9 cells. The 6X His-P10-HA was incubated with a glutathione-agarose purified GST-LsRACK1 or GST tag. The final pull-down products were separated in SDS-PAGE gels and then subjected to Western blot detection with an anti-HA antibody. The 6X His-P10-HA was detected only when both 6X His-P10-HA and GST-LsRACK1 were present in the reaction, further confirming that LsRACK1 interacted with RBSDV P10 (figure 1*e*).

(b) Minimum domains required for rice black-streaked dwarf virus P10–LsRACK1 interaction

To determine which region(s) in the P10 or the LsRACK1 are responsible for their interaction, seven P10 deletion mutants (muP10-1-270, muP10-240-558, muP10-1-140 and muP10-110-270, muCP1-110, muCP110-140, muCP140-240; figure 2*a*) and six LsRACK1 deletion mutants (muRACK1-1-179, muRACK1-179-315, muRACK1-179-268, muRACK1-220-315, muRACK1-220-268 and muRACK1-268-315; figure 2*b*) were made and cloned into vector pGADT7 and pGBKT7, respectively. Interactions between various P10 and LsRACK1 constructs were investigated by Y2H assays. Results of the assays indicated that co-presence of muP10-1-110, muP10-1-140, or muP10-1-270 and LsRACK1 led to a strong positive reaction (figure 2*c*). This interaction was, however, not observed when muP10-1-270 was replaced with

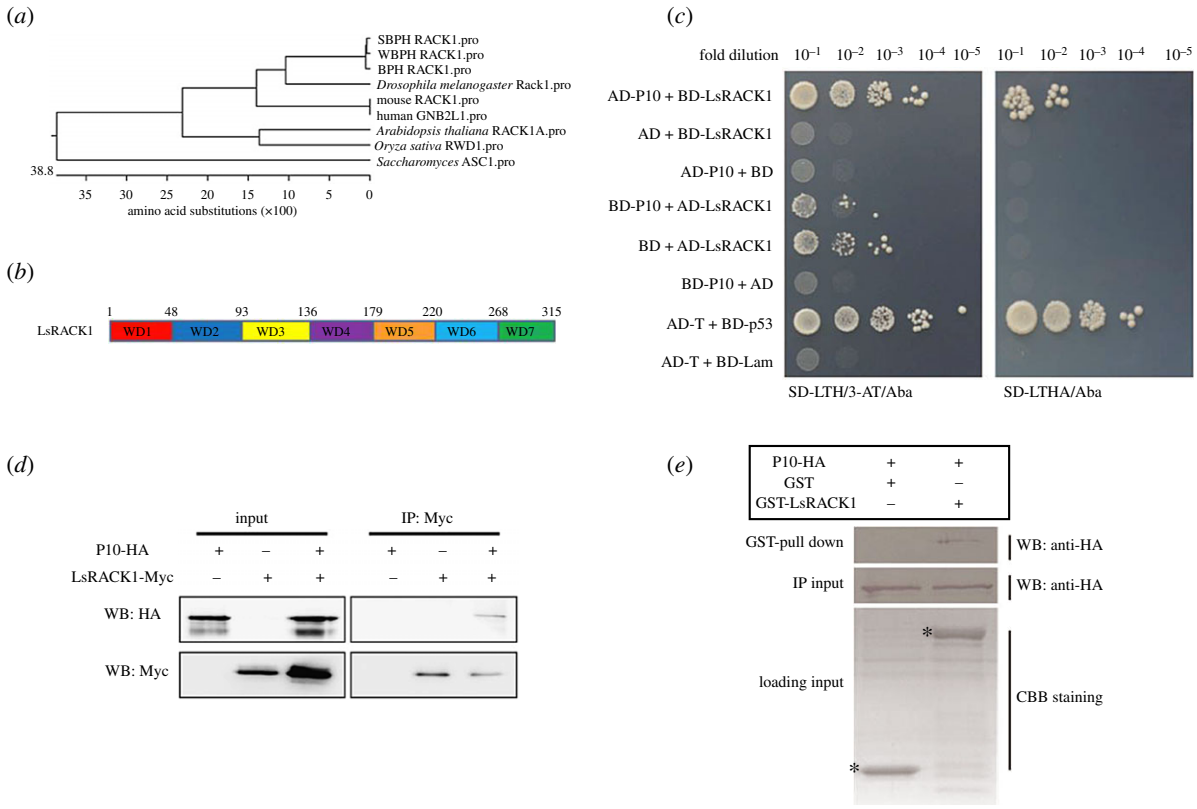

Figure 1. Interaction between RBSDV P10 and LsRACK1. (*a*) Phylogenetic analysis using RACK1 amino acid (aa) sequences from different sources. (*b*) Schematic of RACK1. WD40 domains are short structural motifs with about 40 aa and the numbers above the diagram represent the aa positions. (*c*) Results of yeast two-hybrid assays. RBSDV P10 and LsRACK1 were cloned individually into pGADT7 (AD) and pGBKT7 (BD) vectors. Serial dilutions of yeast cells co-transfected with two various combined vectors were plated on the SD-LTH/3-AT/Aba or SD-LTHA/Aba medium. Cells co-transfected with AD-T and BD-p53 and with AD-T and BD-Lam were, respectively, used as a positive and a negative control. Positive interactions are indicated by the growth of the cells. (*d*) Co-IP. LsRACK1-Myc and P10-HA were separately or co-expressed in Sf9 cells by transfection. LsRACK1-Myc expressed alone in cells served as a negative control. At 48 h post transfection, Sf9 cell lysates were immunoprecipitated with anti-Myc beads followed by Western blot (WB) using an anti-HA (upper panel) or an anti-Myc antibody (lower panel). (*e*) GST pull-down assay. GST or GST-LsRACK1 was incubated with 6X His-P10-HA and then mixed with glutathione-sepharose beads. The beads were washed and analysed by Western blot using an anti-HA antibody (upper panel). The middle panel shows the Western blot results of inputs of HA-tagged P10 proteins from pull-down assays. Equal volume of glutathione-sepharose beads carrying GST-LsRACK1 or GST were analysed by SDS-PAGE and stained with Coomassie blue. The position of GST-LsRACK1 or GST is indicated with asterisks.

muP10-240-558 (figure 2*c*), demonstrating that the P10 N terminal region covering aa 1–270 was responsible for the strong interaction with LsRACK1. muP10-110-270 or muP10-140-240 had a weak interaction with LsRACK1 (figure 2*c*). We then tested various LsRACK1 mutants and determined that mutant muRACK1-1-179, muRACK1-179-268 and muRACK1-220-268 failed to interact with RBSDV P10, while mutant muRACK1-179-315, muRACK1-220-315 and muRACK1-268-315 all gave a strong interaction with RBSDV P10 (figure 2*d*), indicating that the seventh WD40 domain, covering LsRACK1 aa 268–315, is essential for the interaction with RBSDV P10. No positive interaction was observed when individual mutants were co-expressed with empty pGADT7 or pGBKT7 (figure 2*c*,*d*).

(c) Influence of rice black-streaked dwarf virus infection on LsRACK1 expression

We reasoned that the accumulation of RBSDV in viruliferous *L. striatellus* might interfere with the expression of *LsRACK1*. To address this concern, we analysed the temporal and spatial expression pattern of *LsRACK1* in non-viruliferous and viruliferous *L. striatellus* using qRT-PCR. In the non-viruliferous *L. striatellus*, the highest *LsRACK1* expression level was found in the four-instar nymphs while the lowest expression level was found in the adult (figure 3*a*). In adult *L. striatellus*, the highest *LsRACK1* expression was found in testis followed by the ovary, and the lowest expression was found in salivary glands and the gut (figure 3*b*). The expression levels of *LsRACK1* transcript and LsRACK1 protein in the non-viruliferous or viruliferous adult males or females were similar (figure 3*c*,*e*). In various organs, the expression levels of *LsRACK1* were also similar between the non-viruliferous and viruliferous *L. striatellus* (figure 3*d*), indicating that the accumulation of RBSDV had no effect on *LsRACK1* expression in *L. striatellus*.

(d) Rice black-streaked dwarf virus P10 altered the subcellular localization pattern of LsRACK1

Subcellular localization patterns of RBSDV P10 and LsRACK1 were investigated using a baculovirus expression system. RBSDV P10, muP10-1-270 and muP10-240-558 were, respectively, tagged with the eGFP at their C-terminus, and LsRACK1 was tagged with a green or red fluorescent protein at its C-terminus. Under the confocal microscope, P10-eGFP, muP10-1-270-eGFP and ER:mCherry (a maker with an ER retention signal) were found to form granular-like structures

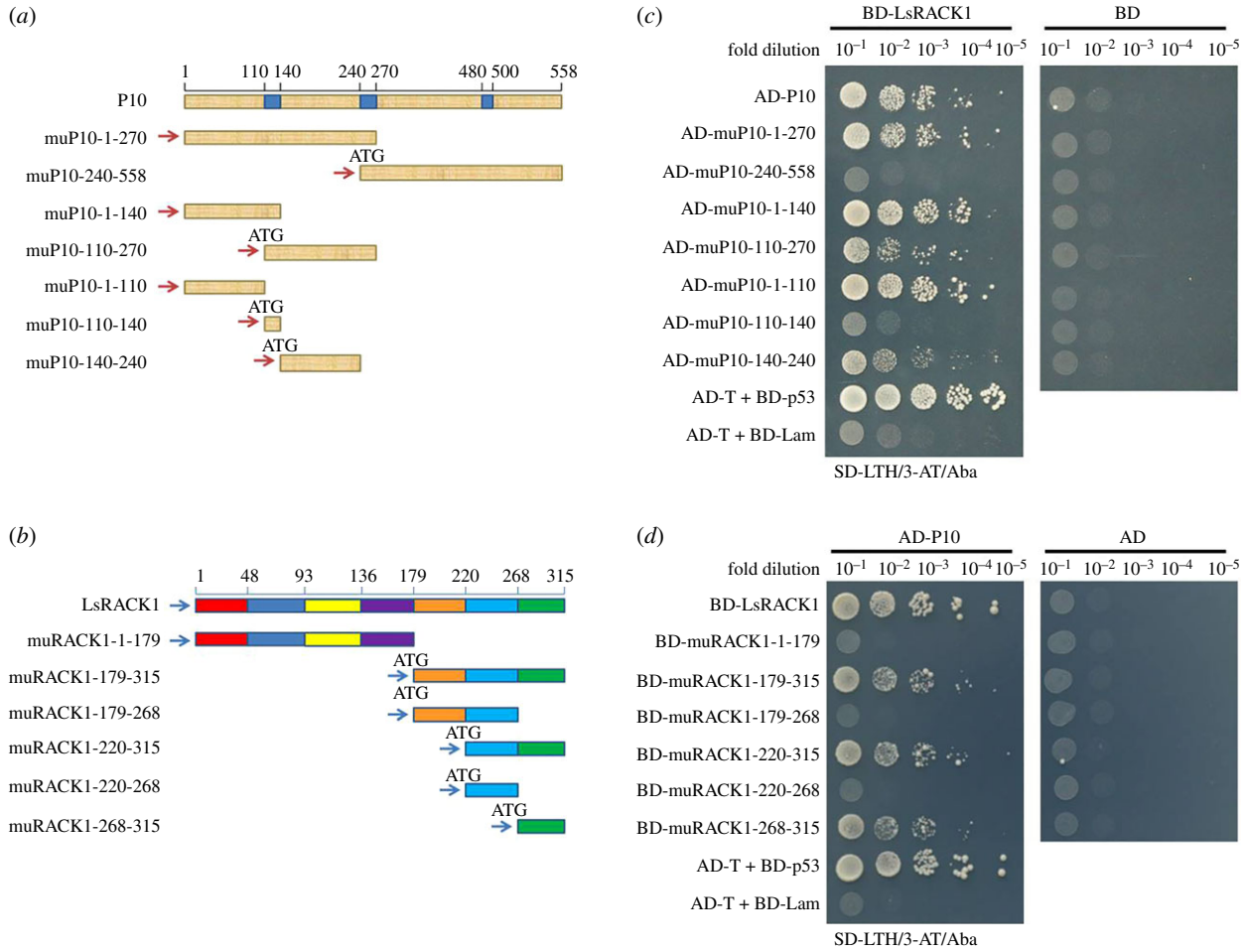

Figure 2. Determination of domains needed for RBSDV P10 and LsRACK1 interaction. (*a*) Schematic of RBSDV P10 and its deletion mutants. The three blue boxes inside the diagram represent transmembrane domains in the RBSDV P10. The numbers above the diagram represent the positions of amino acids. The seven short fragments below the P10 diagram represent the seven deletion mutants and their respective positions. (*b*) Schematic of LsRACK1. Different colours shown in the diagram represent seven WD40 domains, respectively. The fragments below the diagram represent the LsRACK1 deletion mutants. (*c*) Yeast two-hybrid assay results showing the positive or negative interactions between AD-P10 and its deletion mutants with BD-LsRACK1. Co-expression of AD-P10 or its deletion mutants with the BD vector were used as negative controls. (*d*) Yeast two-hybrid assay results showing the positive or negative interactions between BD-LsRACK1 and its deletion mutants with AD-P10. The cell co-expressing AD-T and BD-p53 was used as a positive control, and the cell co-expressing AD-T and BD-Lam was used as a negative control.

in cytoplasm of Sf9 cells while muP10-240-558-eGFP was found to be free in the cells, similar to that shown by the free eGFP (figure 4*a*). Expressing of LsRACK1-eGFP in Sf9 cells also showed granular-like structures in cells (figure 4*a*).

To determine whether these granular-like structures were associated with the ER network, P10-eGFP and ER:mCherry were co-expressed in Sf9 cells. Results of the study showed that co-expression of these two proteins in Sf9 cells yielded co-localized green and red granular-like structures, as indicated by the yellow fluorescent structures in the superimposed image (figure 4*b*, the top image of the right side column). Similar results were obtained when muP10-1-270-eGFP was co-expressed with ER:mCherry in Sf9 cells (figure 4*b*). By contrast, co-expression of LsRACK1-eGFP and ER:mCherry in Sf9 cells did not produce co-localized granular-like structures, in a manner of incomplete overlap, as indicated by the green fluorescent structures in the superimposed image (figure 4*b*, the bottom image of the right side column).

Because co-expression of P10-eGFP and LsRACK1-red fluorescent protein (RFP) in Sf9 cells also resulted in a co-localization pattern with green and red granular-like structures (figure 4*c*), we further analysed the midgut, ovary and testis from viruliferous *L. striatellus* by immunohistochemistry using a mixture of an anti-RBSDV P10 murine monoclonal antibody conjugated with FITC and an anti-LsRACK1 rabbit polyclonal antibody followed by a goat anti-rabbit IgG conjugated with Alexa Flour 555. Results of the assays indicated that the tissues which had accumulated RBSDV P10 also accumulated high-level LsRACK1, leading to a co-localized green and red florescence pattern (figure 5). We further analysed the ovary proteins from viruliferous or non-viruliferous *L. striatellus* by Western blot using an anti-RBSDV P10 monoclonal antibody, and the result proved further that P10 can be localized on the ovary of the viruliferous *L. striatellus* (electronic supplementary material, figure S1), which was consistent with the result of immunohistochemistry (figure 5).

To further support our above results, a membrane flotation assay was conducted to show that RBSDV P10 could alter LsRACK1 distribution in cells. Sf9 cells were lysed in a hypotonic buffer at 48 h post-transfection and the lysates were separated by ultra-centrifugation and analysed by Western blot using specific antibodies. Results indicated that cell membrane-associated proteins were enriched in the 10% sucrose gradient fractions and the membrane vesicles, as well as RBSDV P10, were mainly present in the 65% sucrose gradient fractions close to the last 10% sucrose gradient fraction

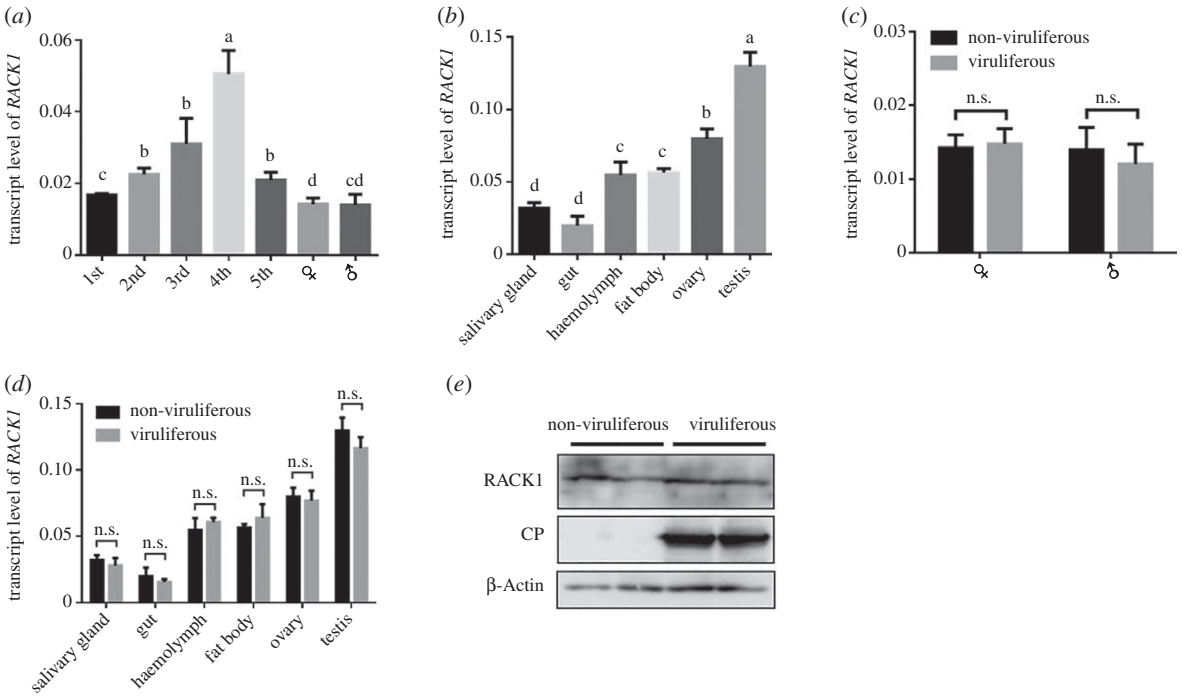

Figure 3. Expression pattern of *LsRACK1* in *L. striatellus*. (*a*) Relative expression levels of *LsRACK1* in non-viruliferous *L. striatellus* at various developmental stages. (*b*) Relative expression levels of *LsRACK1* in various tissues of non-viruliferous *L. striatellus*. (*c*) Relative expression levels of *LsRACK1* in viruliferous and non-viruliferous female or male *L. striatellus*. (*d*) Relative expression levels of *LsRACK1* in various tissues of viruliferous and non-viruliferous *L. striatellus*. All the results of figures *a*–*d* were determined by qRT-PCR using *LsRACK1*-specific primers and were normalized against the expression level of *L. striatellus* β-Actin gene. Each bar represents the mean of three biological repeats. Different lowercase letters above the bars indicate a significant statistical difference between the treatments. n.s., no significant statistical difference determined by the Tukey's multiple comparison tests ($p > 0.05$). (*e*) Western blot assay showing LsRACK1 and RBSDV P10 accumulation in adult viruliferous and non-viruliferous *L. striatellus*. The proteins were probed with an anti-RACK1, an anti-RBSDV P10, or an anti β-Actin antibody, respectively. The expression of *L. striatellus* β-Actin was used as a control.

(figure 4*d*). To validate the separation efficiency, individual fractions were also analysed for the presence of eGFP and ER:mCherry. As expected, eGFP was remained predominantly in the 80% sucrose gradient fractions while ER:mCherry was mostly in the 65% sucrose gradient fractions, owing mainly to its association with the membrane through its histidine-aspartic acid-glutamate-leucine sequence (the two upmost panels in figure 4*d*). The enrichment of LsRACK1-eGFP in 65% sucrose gradient fractions, in the presence of P10-HA or muP10-1-270-HA, indicated that the presence of RBSDV P10 in Sf9 cells altered LsRACK1 migration pattern during gradient centrifugation. Together with the above subcellular localization results, we conclude that the ER membrane-associated RBSDV P10 captures cytosolic LsRACK1 in granular-like forms through protein–protein interaction.

(e) Silencing LsRACK1 expression in *Laodelphax striatellus* enhanced rice black-streaked dwarf virus accumulation

To investigate whether *LsRACK1* is important for RBSDV accumulation in *L. striatellus*, we knocked down the expression level of *LsRACK1* in *L. striatellus* through *LsRACK1*-dsRNA microinjection. The microinjected *L. striatellus* nymphs were analysed for *LsRACK1* expression by qRT-PCR. Results showed that the expression level of *LsRACK1* in *LsRACK1*-dsRNA-injected nymphs decreased by about 94.9% compared with the *gfp*-dsRNA-injected nymphs at 48 hpi (figure 6*a*). Results of Western blot analyses agreed with the results from qRT-PCR assays and showed that a very low amount of LsRACK1 had accumulated in the *LsRACK1*-silenced *L. striatellus* nymphs at 48 hpi (figure 6*b*). Because the survival rate of the *LsRACK1*-silenced *L. striatellus* nymphs was similar to that of the *gfp*-dsRNA-injected nymphs (control, figure 6*c*), we speculated that the expression of *LsRACK1* might not have significant roles in *L. striatellus* growth and development. In a separate experiment, *LsRACK1*-silenced or *gfp*-dsRNA-injected *L. striatellus* nymphs were allowed to feed on RBSDV-infected rice plants for 3 d and then transferred to healthy rice seedlings for 15 d followed by qRT-PCR using RBSDV P10 specific primers. Results of the assay demonstrated that, compared with the *gfp*-dsRNA-injected *L. striatellus* nymphs, much higher RBSDV accumulation was found in the *LsRACK1*-silenced nymphs (figure 6*d*).

(f) Rice black-streaked dwarf virus infection impaired protein kinase C activity in *Laodelphax striatellus*

Previous reports have indicated that virus infection could affect host PKC activities [39–41], leading to an increased or reduced phosphorylation of various substrates and then influence cellular functions. In this study, we first evaluated the impact of LsRACK1 on PKC activities. Second-instar *L. striatellus* nymphs were microinjected with *LsRACK1*-dsRNA or *gfp*-dsRNA, and then placed on healthy rice seedlings for 2 d. Analyses using total protein from *L. striatellus* demonstrated that the activities of PKCs in the *LsRACK1*-silenced *L. striatellus* was significantly reduced compared with that of *gfp*-injected *L. striatellus* (figure 6*e*). To further confirm this finding, we analysed PKC activity of the crude extracts from uninfected or RBSDV-infected *L. striatellus*. Results shown in figure 6*f*

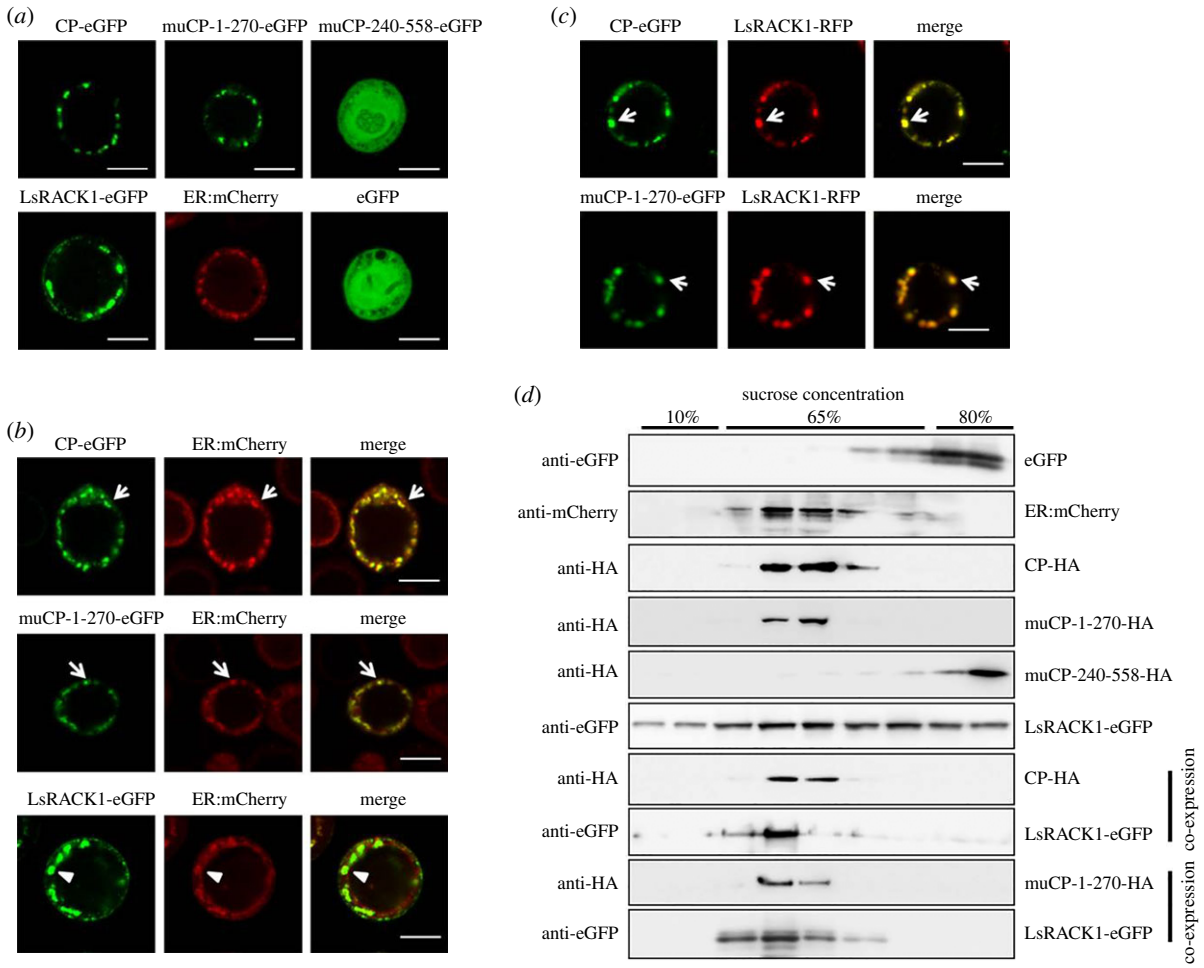

Figure 4. Expression of RBSDV P10 altered the subcellular localization pattern of LsRACK1. (*a*) Subcellular localization of P10-eGFP, muP10-1-270-eGFP, muP10-240-558-eGFP, ER:mCherry and LsRACK1-eGFP in Sf9 cells. The eGFP-expressed cell was used as a control. The transfected Sf9 cells were examined by confocal microscopy at 48 h post-transfection. Scale bars, 10 μm. (*b*) Sf9 cells were co-transfected with ER:mCherry and P10-eGFP, muP10-1-270-eGFP or LsRACK1-eGFP. The transfected cells were examined under a confocal microscope. The images were then processed using ZEISS ZEN confocal microscope software. White arrows indicate the granules of ER:mCherry, P10-eGFP or muP10-1-270-eGFP. The white arrows indicate the co-localized granules (yellow colour) in the superimposed images. Expressed LsRACK1 also formed granules (white arrowhead) in cells, which did not co-localize with ER:mCherry formed granules (white arrowhead). Scale bars, 10 μm. (*c*) Co-expression of P10-eGFP or muP10-1-270-eGFP with LsRACK1-RFP in Sf9 cells. Results of the assays indicated that the granules formed by P10-eGFP or muP10-1-270-eGFP co-localized with the granules formed by LsRACK1-RFP (white arrows). Scale bars, 10 μm. (*d*) Membrane flotation assays. After sucrose gradient centrifugation, proteins were separated in SDS-PAGE gels followed by a Western blot analysis using specific antibodies, namely anti-GFP, anti-mCherry and anti-HA antibody. Each experiment was repeated three times and similar results were obtained.

indicated that the activity of PKCs in the extract from RBSDV-infected *L. striatellus* was significantly decreased compared with that in the extract from the uninfected *L. striatellus*.

(g) Expression of rice black-streaked dwarf virus P10 in *Spodoptera frugiperda* 9 cell impaired the activities of PKCs

RACK1 is known as a receptor of PKCs and a multifunctional scaffold protein involved in many important signal transduction pathways. To further determine if interaction between RBSDV P10 and LsRACK1 affects the activities of PKCs in *L. striatellus*, we analysed the activities of PKCs in the P10-, muP10-1-270- or muP10-240-558-transfected Sf9 cells harvested at 2 dpi. Results indicated that the activities of PKCs in the P10, or muP10-1-270-transfected Sf9 cells were significantly reduced compared with the *gfp*-transfected control cells (figure 6*g*). By contrast, in the muP10-240-558-transfected Sf9 cells, the activities of PKCs remained unchanged (figure 6*g*). It is noteworthy that the expression levels of GFP, P10 or P10 mutants in each treatment were similar to that determined by Western blot (figure 6*h*).

(h) Protein kinase C activities negatively regulated rice black-streaked dwarf virus accumulation

To further determine the role of PKCs during RBSDV replication, PKCs specific inhibitor (10 μl 1 μM Calphostin C) or PKCs activator (10 μl 1 μM PMA) was injected into *L. striatellus*. *Laodelphax striatellus* injected with 1% dimethyl sulfoxide (DMSO) was used as a control. The activities of PKCs in the Calphostin C-injected *L. striatellus* decreased approximately 64.2% compared with the control *L. striatellus*. By contrast, a 22.8% increase of PKCs activities was observed in the PMA-injected *L. striatellus* at 24 hpi (figure 7*a*). In this assay, the survival rate of injected *L. striatellus* was compared, and the result indicated that Calphostin C and PMA had no significant effect on *L. striatellus* viability (figure 7*b*). We then analysed the effect of PKCs activities on the accumulation of RBSDV P10 by qRT-PCR. The results demonstrated that the

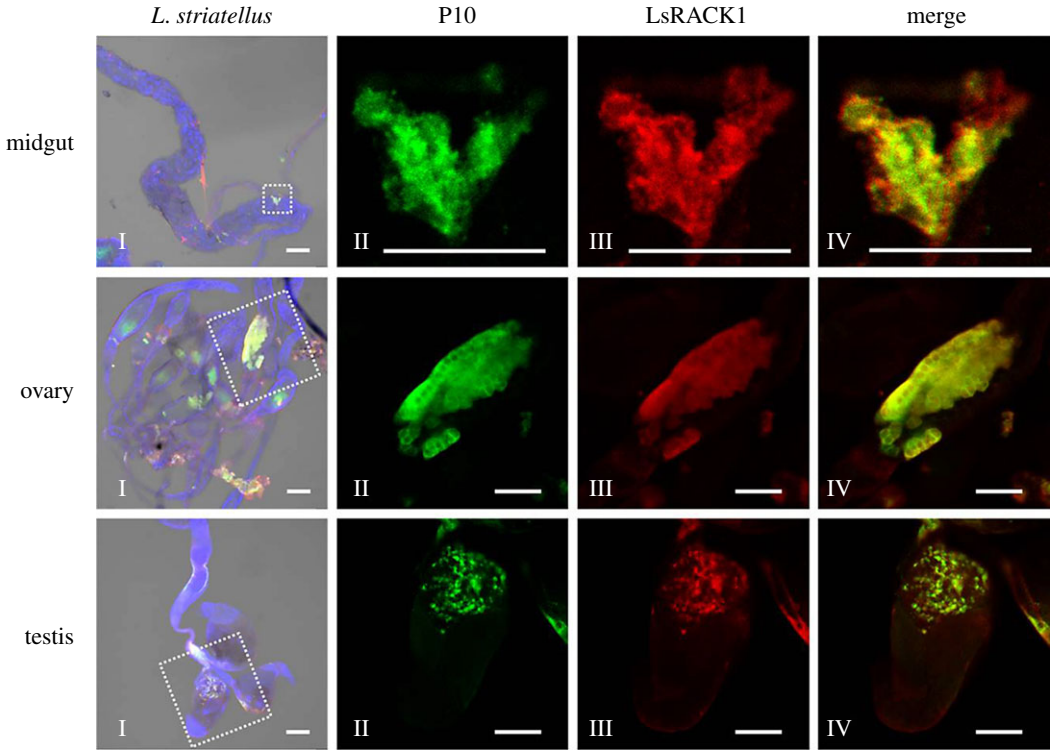

Figure 5. Immunocytochemical detection of RBSDV P10 and LsRACK1 in different organs of RBSDV-infected *L. striatellus*. Midguts, ovaries and testes were separated from viruliferous *L. striatellus*, and immunostained with a mixture of an anti-RBSDV P10 murine monoclonal antibody conjugated with FITC and an anti-LsRACK1 rabbit polyclonal antibody followed by a goat anti-rabbit IgG conjugated with Alexa Flour 555. The labelled tissues were examined under a confocal microscope. Nuclei in cells were stained blue using DAPI. Images in the left column (Is) were merged and low magnification images show the labelling signal in whole tissues. Images in the middle two columns (IIs and IIIs) are enlarged images from the boxed regions inside the I column images. Accumulation of RBSDV P10 was indicated by the green florescence from FITC and the accumulation of LsRACK1 was indicated by the red florescence from Alexa Fluor 555. Images in the right column (IVs) were the enlarged superimposed images. Images shown in this figure are representative images from the assay. Scale bars, 50 μm.

Calphostin C-injection treatment caused an increase of virus accumulation in *L. striatellus* while the PMA-injection treatment negatively affected the accumulation of RBSDV (figure 7*c*).

4. Discussion

It is well known that the capsid protein of viruses plays an important role in vector transmission of viruses. Deciphering the function and mechanism of RBSDV P10 involved in the process of RBSDV transmission by *L. striatellus* is important to uncover the epidemic tendency and establish a scientific system for prevention and control of RBSDV.

Insect transmission of plant viruses needs interactions between viral proteins and vector factors [8,29,42,43]. Consequently, characterization of viral proteins that interact with specific vector factors and understanding how viruses combat vector defence systems during their replication and movement in their insect vectors will provide important evidence and knowledge for developing new strategies for virus disease management. Rice stripe virus (RSV)-*L. striatellus* interaction is the most widely studied case for planthopper-borned viruses. Huo *et al.* [44] reported that RSV could use a vector transovarial transportation system for its transovarial transmission, and the vitellogenin (Vg) of *L. striatellus* played a critical role in this process [44]. In another report, RSV was reported to manipulate the c-Jun N-terminal kinase (JNK) signalling pathway in *L. striatellus* and the activation of JNK promoted RSV replication in its vector [38]. Further study revealed that the coat protein of RSV competitively bound with the G protein pathway suppressor 2 (GPS2) to release GPS2 from inhibiting the activation of the JNK signalling pathway [38].

RACK1, also known as guanine nucleotide-binding protein subunit beta-2-like 1 (GNB2L1) in humans, is a scaffold protein composed of seven WD40 domains and is involved in a variety of signalling transductions. The WD repeat sequence in RACK1 is highly conserved in a diverse range of species, including plants [45], and genetically malleable species such as *Drosophila melanogaster* [46]. The LsRACK1 identified in this study shears the highest amino acid sequence identity (81.6%) with that of *D. melanogaster* followed by human and mouse (figure 1*a*). We also amplified the *RACK1* gene from the white-backed planthopper (*Sogatella furcifera*) and brown planthopper (*Nilaparvata lugens*) and found that their amino acid homology reached 99.7% and 99.4% with that of *L. striatellus*, respectively. RACK1 is known to be ubiquitously expressed in tissues of higher mammals and humans [47,48]. In this study, qRT-PCR analyses revealed that *LsRACK1* expressed in all tested tissues of *L. striatellus* at different levels, suggest that it may have an important functional role in most, if not all, cells.

The RACK1 of aphid vector, *M. persicae*, can bind with wild-type BWYV virion, but much less efficiently with virions of two BWYV mutants during virus endocytosis/transcytosis, suggesting that RACK1 may play a key role in the process of virus endocytosis/transcytosis [32]. Although the interaction between RSV virion and LsRACK1 has been reported previously [31], which protein of RSV interacts with LsRACK1 was unknown. Results from this study demonstrated for the first time to our knowledge, that RBSDV P10 interacted directly with the LsRACK1 of *L. striatellus*. Further study showed that

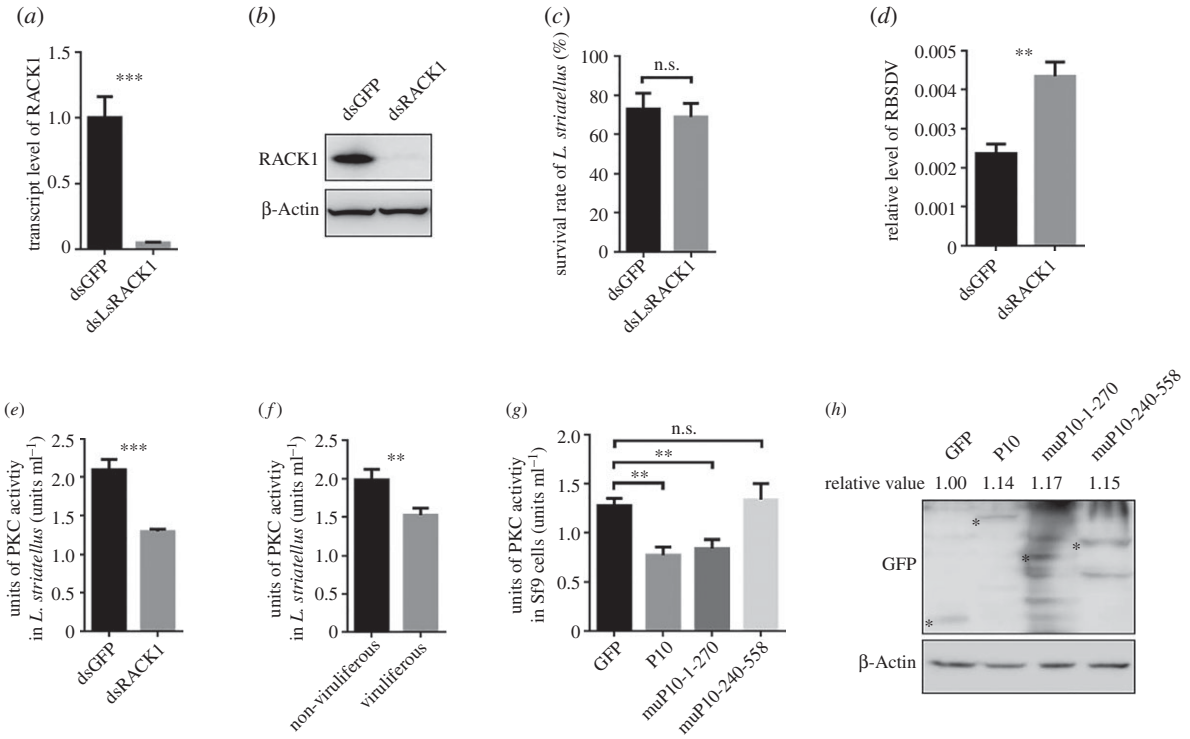

Figure 6. LsRACK1 negatively regulated RBSDV accumulation in *L. striatellus* through suppressing the PKC signalling pathway. (*a*) Relative expression level of *LsRACK1* in *LsRACK1*-dsRNA or *gfp*-dsRNA-microinjected *L. striatellus* at 48 h post-injection (hpi). Results were the means of 30 *L. striatellus* per treatment. (*b*) Western blot analysis of LsRACK1 in *LsRACK1*-dsRNA or *gfp*-dsRNA-microinjected *L. striatellus* at 48 hpi. The lower panel shows the accumulation of β-Actin and is used to show sample loadings. (*c*) Survival rates of *LsRACK1*-dsRNA or *gfp*-dsRNA-microinjected *L. striatellus* at 24 hpi. (*d*) Relative accumulation levels of RBSDV P10 in *LsRACK1*-dsRNA or *gfp*-dsRNA-microinjected *L. striatellus* at 15 d post virus acquisition. (*e*) Activities of PKC kinase in *LsRACK1*-dsRNA or *gfp*-dsRNA-microinjected *L. striatellus*. Thirty *L. striatellus* were used in each treatment. (*f*) Activities of PKC kinase in non-viruliferous and viruliferous *L. striatellus*. Each treatment had 30 *L. striatellus*. (*g*) PKC kinase activities in Sf9 cells expressing RBSDV P10, muP101-270, muP10-240-558 or eGFP. Bars in (*a*–*g*) are the means of three biological replicates ± s.d. $*p < 0.05$; $**p < 0.01$; $***p < 0.001$; n.s., not significant difference ($p > 0.05$). (*h*) Western blot analyses of RBSDV P10-eGFP, muP10-1-270-eGFP, muP10-240-558-eGFP or eGFP expressed in Sf9 cells. The experiments presented in this figure were repeated three times. The relative expression levels of GFP, CP or CP mutants in each treatment were quantified using ImageJ software (https://imagej.nih.gov/ij/). Mean values of target were obtained after normalizing to β-Actin control and the protein accumulation of GFP was set as standard '1'.

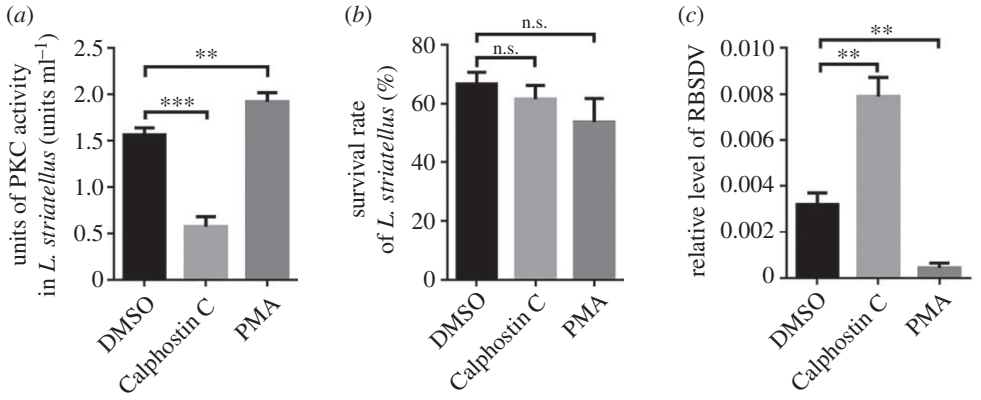

Figure 7. Inhibition of PKC activity enhanced RBSDV accumulation in *L. striatellus*. (*a*) Activities of PKC kinase in *L. striatellus* treated with DMSO, Calphostin C or PMA at 24 hpi. The assay was conducted using the PepTag® non-radioactive PKC assay kit (Promega). Each treatment had 30 *L. striatellus*. (*b*) Survival rate of *L. striatellus* injected with Calphostin C, PMA or 1% DMSO (control) was measured by counting the survival insects at 24 hpi. Each bar represents the mean of 30 *L. striatellus* per treatment ± s.d. (*c*) Relative accumulation level of RBSDV RNA in Calphostin C-, PMA- or DMSO-injected *L. striatellus* at 15 d post-RBSDV acquisition. The accumulation was determined through qRT-PCR using a set of P10 specific primers. The bars represent the mean of three biological repetitions per treatment ± s.d. $*p < 0.05$; $**p < 0.01$; $***p < 0.001$; n.s., not significant ($p > 0.05$). All the experiments were repeated three times and similar results were obtained.

the seventh WD 40 domain at the C terminus (aa 268–315) of LsRACK1 and the N terminus (aa 1–270) of RBSDV P10 are critical for the interaction between RBSDV P10 and LsRACK1. Earlier reports have also indicated that human RACK1 was localized at the internal side of membranes and on cytoskeletons in cytosol [22,23]. It was also reported that the C terminus of RACK1 interacted with various signal transduction components and brought these components into stable complexes [49]. Particularly, the sixth WD 40 domain is responsible for binding with and activating PKC both *in vitro* and *in vivo* [20,23]. Moreover, the correct localization of RACK1 was important for its biological function [22,23]. ER is known

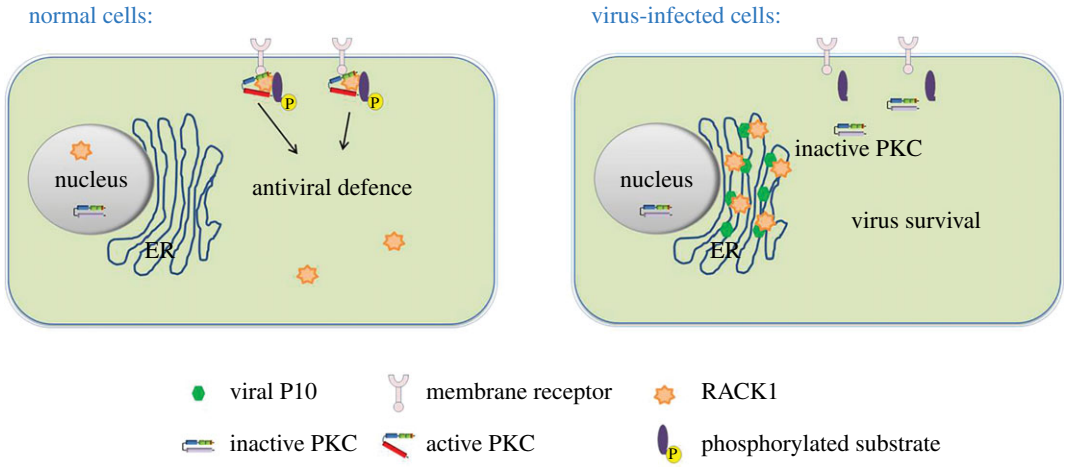

Figure 8. Model of RBSDV regulating PKC signalling pathway in *L. striatellus* to increase its replication. The PKC pathway participates in antiviral defence in *L. striatellus*. RBSDV P10 is synthesized on ER membranes and forms ER membrane-associated granules. RBSDV P10 brings LsRACK1, and makes it located on ER membranes through protein–protein interaction. The altered LsRACK1 conformation leads to an impaired PKC activity in RBSDV-infected *L. striatellus* cells.

to be the major site for protein synthesis and the accumulation of RBSDV P10 was reported to associate with ER in plant cells [11].

We found that LsRACK1 appeared in both cytoplasm and the cell membrane as small granules when expressed alone in Sf9 cells, while RBSDV P10 was co-expressed with LsRACK1 in cells, the interaction between the two proteins resulted in co-localized granules in or associated with ER, suggesting that RBSDV P10 interacted with LsRACK1 and brought it to the ER. We also found that the interaction between RBSDV P10 and the seventh WD 40 domain changed the subcellular localization pattern of LsRACK1. This new finding shades a new light on the special function of RBSDV P10 during virus transmission and infection in its vector.

DsRNA-induced gene silencing through microinjection has been widely used to down-regulate gene expression in planthoppers [36,50]. Our experimental results demonstrated that knockdown of *LsRACK1* gene expression in *L. striatellus* through microinjection did not cause obvious morphological changes and death of the insect. In a different study, we determined that the accumulation of RBSDV was significantly increased after silencing *LsRACK1* gene expression in *L. striatellus*. Thus, we consider that *LsRACK1* is an antiviral gene in *L. striatellus*, and possibly in other insect vectors too, but has no significant role in *L. striatellus* growth and development. RACK1 is a receptor for activated C-kinase and responsible for binding with active forms of PKC family enzymes. We found that the PKC activity in the RBSDV-infected *L. striatellus* was much lower than that in the non-viruliferous *L. striatellus*. Moreover, the PKC activity in Sf9 cells expressing RBSDV P10 or a P10 N terminus deletion mutant, i.e. muP10-1-270 was significantly lower than that in the control Sf9 cells expressing GFP only. Those study results indicated that expression of RBSDV P10 could down-regulate activities of PKCs, a downstream signalling molecule of the RACK1 pathway. Further study found that inhibition of PKC activity using specific inhibitor Calphostin C significantly enhanced RBSDV accumulation in vectors, whereas activation of PKC using activator PMA dramatically inhibited RBSDV accumulation. Therefore, we think that the PKC pathway is important for the antivirus response in *L. striatellus*. Thus, we speculate that the decrease of PKC activity in viruliferous insects is a result caused by the interaction between RBSDV P10 and LsRACK1 that changes the subcellular localization and function of LsRACK1.

Our speculation is supported by a precious study showing that the ZEBRA protein of Epstein-Barr virus (EBV) could bind with RACK1 *in vitro*, and EBV infection altered the subcellular localization of RACK1 and impaired the activity and translocation of PKCα/β in infected monocytes [51]. Such disruption of PKC translocation/activation contributed to the ability of the EBV ZEBRA protein to interact with RACK1 [39]. Moreover, the HIV-1 Nef protein binds with RACK1 and interferes with PKCθ activity in T lymphocytes [51,52]. Thus, disruption of association between PKC and RACK1 can significantly affect PKC activity. Taken together, we propose that during virus infection, virus-encoded protein(s) interacts with RACK1 to suppress PKC activities leading to a weakened downstream antivirus defence response. Our detailed study showed that the N terminus 270 aa of RBSDV P10 is the key region for the interaction between the P10 and LsRACK1. Consequently, this region has the function to regulate the antiviral defence response of insect vectors, like phagocytosis.

Recently, RACK1 was identified as the first plant mitogen-activated protein kinase (MAPK) scaffold protein that connected heterotrimeric G protein with a MAPK cascade to form a unique signalling pathway in plant immunity [53]. Rice is known to contain two *RACK1* genes: *RACK1A* and *RACK1B*. RACK1A has also been identified as an interactor with Rac1, a small GTPase, which is also known as Ras-related C3 botulinum toxin substrate 1, and involved in rice innate immunity [54]. The study also found that Rac1 regulated the expression of RACK1A at both transcriptional and post-transcriptional levels [54]. Transcription of *RACK1A* can be induced by a fungal elicitor or by abscisic acid, jasmonate and auxin, respectively [54]. *RACK1A* also plays a role in the production of reactive oxygen species and in disease resistance against rice blast infection [55]. Together, RACK1 is involved in blocking the release of the virus particle, activation of MAPK which controls antiviral responses, cell survival, proliferation and cell viability [53,56].

In summary, our findings presented here provide new evidence showing that the N-terminus region of RBSDV P10 is responsible for impairing the innate immunity in *L. striatellus*, and this function is achieved through altering the subcellular location pattern of LsRACK1 and modulating the structure and function of PKC in its vector. Therefore, we provide a

model to summarize how RBSDV manipulates the PKC signalling pathway to increase its replication in *L. striatellus* (figure 8). We consider that LsRACK1 and the PKC pathway play critical roles in antiviral defence in *L. striatellus* and other insect vectors. This new finding sheds new light on the special function of RBSDV P10 during virus transmission and infection, and should contribute to our knowledge on the mechanisms controlling RBSDV transmission through *L. striatellus*.

Data accessibility. Additional data is supplied as the electronic supplementary material.

Authors' contribution. J.W. and X.Z. conceived and designed the study, secured funding and contributed to data analysis; L.L. and Q.W. conducted laboratory work and drafted the paper. D.H. and Q.X. performed assays and contributed to data analysis. All the authors contributed to manuscript revisions and gave their final approval for publication.

Competing interests. We declare we have no competing interests.

Funding. This work was supported by the National Natural Science Foundation of China (nos. 31571976; 31471768), the National Basic Research Program (973) of China (2014CB138400), the National Key Research and Development Project of China (no. 2016YFD0300706), the Earmarked Fund for Modern Agro-industry Technology Research System (nycytx-001) and Dabeinong Funds for Discipline Development and Talent Training in Zhejiang University.

Acknowledgements. We thank Dr Xinshun Ding, Plant Biology Division, the Samuel Roberts Noble Foundation, Oklahoma, USA, (retired) for his comments and language editing on the manuscript. The authors also thank Dr Yijun Zhou, the Institute of Plant Protection, Jiangsu Academy of Agricultural Sciences, China, for providing *L. striatellus* populations.

References

1. Zhang P, Mar TT, Liu W, Li L, Wang X. 2013 Simultaneous detection and differentiation of rice black streaked dwarf virus (RBSDV) and southern rice black streaked dwarf virus (SRBSDV) by duplex real time RT-PCR. *Virol. J.* **10**, 24. (doi:10.1186/1743-422X-10-24)
2. Yin X, Zheng FQ, Tang W, Zhu QQ, Li XD, Zhang GM, Liu HT, Liu BS. 2013 Genetic structure of rice black-streaked dwarf virus populations in China. *Arch. Virol.* **158**, 2505–2515. (doi:10.1007/s00705-013-1766-8)
3. Azuhata F, Uyeda I, Kimura I, Shikata E. 1993 Close similarity between genome structures of rice black-streaked dwarf and maize rough dwarf viruses. *J. Gen. Virol.* **74**, 1227–1232. (doi:10.1099/0022-1317-74-7-1227)
4. Firth AE, Atkins JF. 2009 Analysis of the coding potential of the partially overlapping 3′ ORF in segment 5 of the plant fijiviruses. *Virol. J.* **6**, 32. (doi:10.1186/1743-422X-6-32)
5. Isogai M, Uyeda I, Lee BC. 1998 Detection and assignment of proteins encoded by rice black streaked dwarf fijivirus S7, S8, S9 and S10. *J. Gen. Virol.* **79**, 1487–1494. (doi:10.1099/0022-1317-79-6-1487)
6. Zhang LD, Wang ZH., Wang XB, Zhang WH, Li DW, Han CG, Zhai YF, Yu JL. 2005 Two virus-encoded RNA silencing suppressors, P14 of beet necrotic yellow vein virus and S6 of rice black streak dwarf virus. *Chin. Sci. Bull.* **50**, 305–310. (doi:10.1007/BF02897570)
7. Gallina A, Rossi F, Milanesi G. 2001 Rack1 binds HIV-1 Nef and can act as a Nef-protein kinase C adaptor. *Virology* **283**, 7–18. (doi:10.1006/viro.2001.0855)
8. Liu Y, Jia D, Chen H, Chen Q, Xie L, Wu Z, Wei T. 2011 The P7-1 protein of southern rice black-streaked dwarf virus, a fijivirus, induces the formation of tubular structures in insect cells. *Arch. Virol.* **156**, 1729–1736. (doi:10.1007/s00705-011-1041-9)
9. Zhang C, Liu Y, Liu L, Lou Z, Zhang H, Miao H, Hu X, Pang Y, Qiu B. 2008 Rice black streaked dwarf virus P9-1, an α-helical protein, self-interacts and forms viroplasms *in vivo*. *J. Gen. Virol.* **89**, 1770–1776. (doi:10.1099/vir.0.2008/000109-0)
10. Maroniche GA, Mongelli VC, Llauger G, Alfonso V, Taboga O, del Vas M. 2012 *In vivo* subcellular localization of Mal de Río Cuarto virus (MRCV) non-structural proteins in insect cells reveals their putative functions. *Virology* **430**, 81–89. (doi:10.1016/j.virol.2012.04.016)
11. Sun Z, Yang D, Xie L, Sun L, Zhang S, Zhu Q, Li J, Wang X, Chen J. 2013 Rice black-streaked dwarf virus P10 induces membranous structures at the ER and elicits the unfolded protein response in *Nicotiana benthamiana*. *Virology* **447**, 131–139. (doi:10.1016/j.virol.2013.09.001)
12. Weber PH, Bujarski JJ. 2015 Multiple functions of capsid proteins in (+) stranded RNA viruses during plant-virus interactions. *Virus Res.* **196**, 140–149. (doi:10.1016/j.virusres.2014.11.014)
13. Lavine MD, Strand MR. 2001 Surface characteristics of foreign targets that elicit an encapsulation response by the moth *Pseudoplusia includens*. *J. Insect. Physiol.* **47**, 965–974. (doi:10.1016/S0022-1910(01)00071-3)
14. Lavine MD, Strand MR. 2002 Insect hemocytes and their role in immunity. *Insect Biochem. Mol. Biol.* **32**, 1295–1309. (doi:10.1016/S0965-1748(02)00092-9)
15. Marmaras VJ, Lampropoulou M. 2009 Regulators and signalling in insect haemocyte immunity. *Cell. Signal.* **21**, 186–195. (doi:10.1016/j.cellsig.2008.08.014)
16. Sim S, Dimopoulos G. 2010 Dengue virus inhibits immune responses in *Aedes aegypti* cells. *PLoS ONE* **5**, e10678. (doi:10.1371/journal.pone.0010678)
17. McCahill A, Warwicker J, Bolger GB, Houslay MD, Yarwood SJ. 2002 The RACK1 scaffold protein: a dynamic cog in cell response mechanisms. *Mol. Pharmacol.* **62**, 1261–1273. (doi:10.1124/mol.62.6.1261)
18. Sklan EH, Podoly E, Soreq H. 2006 RACK1 has the nerve to act: structure meets function in the nervous system. *Prog. Neurobiol.* **78**, 117–134. (doi:10.1016/j.pneurobio.2005.12.002)
19. Mochly-Rosen D, Khaner H, Lopez J. 1991 Identification of intracellular receptor proteins for activated protein kinase C. *Proc. Natl Acad. Sci. USA* **88**, 3997–4000. (doi:10.1073/pnas.88.9.3997)
20. Ron D, Chen CH, Caldwell J, Jamieson L, Orr E, Mochly-Rosen D. 1994 Cloning of an intracellular receptor for protein kinase C: a homolog of the beta subunit of G proteins. *Proc. Natl Acad. Sci. USA* **91**, 839–843. (doi:10.1073/pnas.91.3.839)
21. Choi DS, Young H, McMahon T, Wang D, Messing RO. 2003 The mouse RACK1 gene is regulated by nuclear factor-kappa B and contributes to cell survival. *Mol. Pharmacol.* **64**, 1541–1548. (doi:10.1124/mol.64.6.1541)
22. Ron D, Jiang Z, Yao L, Vagts A, Diamond I, Gordon A. 1999 Coordinated movement of RACK1 with activated betaIIPKC. *J. Biol. Chem.* **274**, 27 039–27 046. (doi:10.1074/jbc.274.38.27039)
23. Ron D, Mochly-Rosen D. 1995 An autoregulatory region in protein kinase C: the pseudoanchoring site. *Proc. Natl Acad. Sci. USA* **92**, 492–496. (doi:10.1073/pnas.92.2.492)
24. Adams DR, Ron D, Kiely PA. 2011 RACK1, a multifaceted scaffolding protein: structure and function. *Cell Commun. Signal.* **9**, 22. (doi:10.1186/1478-811X-9-22)
25. Wilson CH, Ali ES, Scrimgeour N, Martin AM, Hua J, Tallis GA, Rychkov GY, Barritt GJ. 2015 Steatosis inhibits liver cell store-operated Ca^{2+} entry and reduces ER Ca^{2+} through a protein kinase C-dependent mechanism. *Biochem. J.* **466**, 379–390. (doi:10.1042/BJ20140881)
26. Ali ES, Hua J, Wilson CH, Tallis GA, Zhou FH, Rychkov GY, Barritt GJ. 2016 The glucagon-like peptide-1 analogue exendin-4 reverses impaired intracellular Ca^{2+} signalling in steatotic hepatocytes. *Biochim. Biophys. Acta* **1863**, 2135–2146. (doi:10.1016/j.bbamcr.2016.05.006)
27. Sieczkarski SB, Whittaker GR. 2002 Dissecting virus entry via endocytosis. *J. Gen. Virol.* **83**, 1535–1545. (doi:10.1099/0022-1317-83-7-1535)
28. Dorn GW, Mochly-Rosen D. 2002 Intracellular transport mechanisms of signal transducers. *Annu.*

Rev. Physiol. **64**, 407–429. (doi:10.1146/annurev.physiol.64.081501.155903)

29. Hogenhout SA, Ammarel D, Whitfield AE, Redinbaugh MG. 2008 Insect vector interactions with persistently transmitted viruses. *Annu. Rev. Phytopathol.* **46**, 327–359. (doi:10.1146/annurev.phyto.022508.092135)
30. Blanc S, Drucker M, Uzest M. 2014 Localizing viruses in their insect vectors. *Annu. Rev. Phytopathol.* **52**, 403–425. (doi:10.1146/annurev-phyto-102313-045920)
31. Li S, Xiong R, Wang X, Zhou Y. 2011 Five proteins of *Laodelphax striatellus* are potentially involved in the interactions between rice stripe virus and vector. *PLoS ONE* **6**, e26585. (doi:10.1371/journal.pone.0026585)
32. Seddas P, Boissinot S, Strub JM, Van Dorsselaer A, Van Regenmortel MH, Pattus F. 2004 Rack-1, GAPDH3, and actin: proteins of *Myzus persicae* potentially involved in the transcytosis of beet western yellows virus particles in the aphid. *Virology* **325**, 399–412. (doi:10.1016/j.virol.2004.05.014)
33. Wu J, Ni Y, Liu H, Rao L, Zhou Y, Zhou X. 2013 Development and use of three monoclonal antibodies for the detection of rice black-streaked dwarf virus in field plants and planthopper vectors. *Virol. J.* **10**, 114. (doi:10.1186/1743-422X-10-114)
34. Shen Q, Liu Z, Song F, Xie Q, Hanley-Bowdoin L, Zhou X. 2011 Tomato SISnRK1 protein interacts with and phosphorylates βC1, a pathogenesis protein encoded by a geminivirus beta-satellite. *Plant Physiol.* **157**, 1394–1406. (doi:10.1104/pp.111.184648)
35. Bentham M, Mazaleyrat S, Harris M. 2006 Role of myristoylation and N-terminal basic residues in membrane association of the human immunodeficiency virus type 1 Nef protein. *J. Gen. Virol.* **87**, 563–571. (doi:10.1099/vir.0.81200-0)
36. Xu HJ *et al.* 2015 Two insulin receptors determine alternative wing morphs in planthoppers. *Nature* **519**, 464–467. (doi:10.1038/nature14286)
37. Huang C, Xie Y, Zhou, X. 2009 Efficient virus-induced gene silencing in plants using a modified geminivirus DNA1 component. *Plant Biotechnol. J.* **7**, 254–265. (doi:10.1111/j.1467-7652.2008.00395.x)
38. Wang W, Zhao W, Li J, Luo L, Kang L, Cui F. 2017 The c-Jun N-terminal kinase pathway of a vector insect is activated by virus capsid protein and promotes viral replication. *Elife* **6**, e26591. (doi:10.7554/eLife.26591)
39. Tardif M, Savard M, Flamand L, Gosselin J. 2002 Impaired protein kinase C activation/translocation in Epstein-Barr virus-infected monocytes. *J. Biol. Chem.* **277**, 24 148–24 154. (doi:10.1074/jbc.M109036200)
40. Park R and Baines JD. 2006 Herpes simplex virus type 1 infection induces activation and recruitment of protein kinase C to the nuclear membrane and increased phosphorylation of lamin B. *J. Virol.* **80**, 494–504. (doi:10.1128/JVI.80.1.494-504.2006)
41. Hartjen P *et al.* 2013 The NTPase/helicase domain of hepatitis C virus nonstructural protein 3 inhibits protein kinase C independently of its NTPase activity. *Cell. Mol. Biol. Lett.* **18**, 447–458. (doi:10.2478/s11658-013-0099-7)
42. Gray S, Gildow FE. 2003 Luteovirus-aphid interactions. *Annu. Rev. Phytopathol.* **41**, 539–566. (doi:10.1146/annurev.phyto.41.012203.105815)
43. Ammar el-D, Tsai CW, Whitfield AE, Redinbaugh MG, Hogenhout SA. 2009 Cellular and molecular aspects of rhabdovirus interactions with insect and plant hosts. *Annu. Rev. Entomol.* **54**, 447–468. (doi:10.1146/annurev.ento.54.110807.090454)
44. Huo Y *et al.* 2014 Transovarial transmission of a plant virus is mediated by vitellogenin of its insect vector. *PLoS Pathog.* **10**, e1003949. (doi:10.1371/journal.ppat.1003949)
45. Kwak JM, Kim SA, Lee SK, Oh SA, Byoun CH, Han JK, Nam HG. 1997 Insulin-induced maturation of *Xenopus oocytes is* inhibited by microinjection of a *Brassica napus* cDNA clone with high similarity to a mammalian receptor for activated protein kinase C. *Planta* **201**, 245–251. (doi:10.1007/s004250050063)
46. Bini L, Heid H, Liberatori S, Geier G, Pallini V, Zwilling R. 1997 Two-dimensional gel electrophoresis of *Caenorhabditis elegans* homogenates and identification of protein spots by microsequencing. *Electrophoresis* **18**, 557–562. (doi:10.1002/elps.1150180337)
47. Guillemot F, Billault A, Auffray C. 1989 Physical linkage of a guanine nucleotide-binding protein-related gene to the chicken major histocompatibility complex. *Proc. Natl Acad. Sci. USA* **86**, 4594–4598. (doi:10.1073/pnas.86.12.4594)
48. Chou YC, Chou CC, Chen YK, Tsai S, Hsieh FM, Liu HJ, Hseu TH. 1999 Structure and genomic organization of porcine RACK1 gene. *Biochim. Biophys. Acta* **1489**, 315–322. (doi:10.1016/S0167-4781(99)00213-4)
49. Wang W *et al*. 2002 Identification and characterization of AGTRAP, a human homolog of murine angiotensin II receptor-associated protein (Agtrap). *Int. J. Biochem. Cell. Biol.* **34**, 93–102. (doi:10.1016/S1357-2725(01)00094-2)
50. Ma Y, Wu W, Chen H, Liu Q, Jia D, Mao Q, Chen Q, Wu Z, Wei T. 2013 An insect cell line derived from the small brown planthopper supports replication of rice stripe virus, a tenuivirus. *J. Gen. Virol.* **94**, 1421–1425. (doi:10.1099/vir.0.050104-0)
51. Baumann M, Gires O, Kolch W, Mischak H, Zeidler R, Pich D, Hammerschmidt W. 2000 The PKC targeting protein RACK1 interacts with the Epstein-Barr virus activator protein BZLF1. *Eur. J. Biochem.* **267**, 3891–3901. (doi:10.1046/j.1432-1327.2000.01430.x)
52. Smith BL, Krushelnycky BW, Mochly-Rosent D, Berg P. 1996 The HIV nef protein associates with protein kinase C theta. *J. Biol. Chem.* **271**, 16 753–16 757. (doi:10.1074/jbc.271.28.16753)
53. Su J, Xu J, Zhang S. 2015 RACK1, scaffolding a heterotrimeric G protein and a MAPK cascade. *Trends Plant Sci.* **20**, 405–407. (doi:10.1016/j.tplants.2015.05.002)
54. Nakashima A *et al.* 2008 RACK1 functions in rice innate immunity by interacting with the Rac1 immune complex. *Plant Cell.* **20**, 2265–2279. (doi:10.1105/tpc.107.054395)
55. Shirasu K, Schulze-Lefert P. 2003 Complex formation, promiscuity and multi-functionality: protein interactions in disease-resistance pathways. *Trends Plant Sci.* **8**, 252–258. (doi:10.1016/S1360-1385(03)00104-3)
56. Daniels CC, Rovnak J, Quackenbush SL. 2008 Walleye dermal sarcoma virus Orf B functions through receptor for activated C kinase (RACK1) and protein kinase C. *Virology* **375**, 550–560. (doi:10.1016/j.virol.2008.01.034)